384 *J. Phys. Chem. A* **2002,** *106,* 384−394

A Computational Study of the Kinetics of the NO_3 Hydrogen-Abstraction Reaction from a Series of Aldehydes (XCHO: X = F, Cl, H, CH_3)

Nelaine Mora-Diez[†] and Russell J. Boyd*

Department of Chemistry, Dalhousie University, Halifax, Nova Scotia, Canada B3H 4J3

Received: July 2, 2001; In Final Form: October 17, 2001

In the present study, ab initio methods are used to study the NO_3 hydrogen-abstraction reaction from a series of aldehydes: FCHO, ClCHO, HCHO, and CH_3CHO. MP2 and BH&HLYP optimizations were carried out, followed by CCSD(T) single point calculations, using the 6-311G(d,p) basis set. Classical transition state theory (TST) is applied for the calculation of the rate constants, and tunneling corrections are considered assuming an unsymmetrical Eckart barrier. The experimental results (activation energy for the CH_3CHO reaction and rate constants for the reaction of NO_3 with HCHO and CH_3CHO) are well reproduced at the CCSD(T)//BH&HLYP level of theory with some corrections. The same level was chosen to predict the remaining unknown kinetic parameters. At this level of calculation the reactions studied were assumed to be elementary.

Introduction

The consequences of the emission of aldehydes into the atmosphere or their formation in the troposphere from the decomposition or oxidation of other pollutants have been the object of several experimental and theoretical studies.[1] It is well known that during the daytime the photolysis of aldehydes and their reaction with OH radicals are the most probable processes.

The OH radical is the key species in the chemistry of the daytime troposphere, since it is the most important oxidant; practically all organic and inorganic compounds are transformed by reaction with OH. The hydroxyl radical is formed mainly from three routes: the photolysis of O_3 and HONO and from the reaction between HO_2 and NO (the most important source under noon-time conditions). In the absence of sunlight the OH radical concentration in the troposphere is very low.[2]

Numerous studies of the reaction of OH with aldehydes have been performed, both experimentally and theoretically.[3,4] Very recent theoretical studies[5] showed the importance of considering the formation of a reactant complex in the kinetics of the OH hydrogen-abstraction reaction from a series of aldehydes (XCHO: X = F, Cl, H, CH_3), at the level of theory chosen (geometries and energies were calculated at the MP2(FC) and CCSD(T) levels of theory, respectively, using the 6-311++G(d,p) basis set). The importance of aldehydes in the chemistry of the polluted atmosphere has been explained elsewhere.[3,5,6] Transition state theory (TST)[7] was applied for the calculation of the rate constants (considering a complex mechanism in which the overall rate depends on the rates of two competitive reactions: a reversible step where a reactant complex is formed, followed by the irreversible hydrogen abstraction to form the products) with successful results. Tunneling corrections were incorporated assuming an unsymmetrical Eckart barrier.[8]

Nitrate radicals were first detected in the stratosphere in 1978[9] and two years later were observed in the troposphere.[10] This free radical, as well as the OH radical, is a strong oxidizing agent and reacts with a number of other atmospheric species.[11] The reaction of NO_3 radicals with atmospheric organic molecules can lead to the formation of undesirable compounds such as HNO_3,[12] peroxyacyl nitrates (PANs),[13] and dinitrates.[14] The only primary source of NO_3 in the troposphere requires the simultaneous presence of NO_2 and O_3 in the same airmass,[2] but during the daytime NO_3 radicals photolize rapidly, thus its presence in the troposphere is significant only in the nighttime. Measurements made over the past 15 years show nighttime NO_3 concentrations near ground level over continental areas ranging up to 1.7×10^{-4} mol L^{-1} (1.0×10^{10} molecule cm^{-3}).[11] It has been mentioned that just as the OH radicals control the chemistry of the daytime atmosphere, NO_3 radicals have the same role in the nighttime.[15] Thus we should expect the reaction with NO_3 radicals to be an important nighttime tropospheric removal route for aldehydes, as has already been mentioned elsewhere.[16] The reaction of NO_3 radicals with unsaturated organic compounds (alkenes, halogenated alkenes, alcohols, terpenes) is also known to represent an important sink for these species in the nighttime troposphere, and a number of experimental and theoretical studies have been performed in this direction.[17] Experimental studies on the reaction between alkanes, aliphatic alcohols, and ethers with NO_3 radicals have also been performed.[14,18]

There have been fewer kinetic studies on the reactions of NO_3 with aldehydes than on the corresponding reactions with OH radicals. The explanation may be due to differences in the reactivities of these two oxidant radicals, among other factors, as discussed below. Several experimental kinetic studies on the reactions between NO_3 radicals and aliphatic aldehydes (C_1−C_4, and certain C_5 and C_6 aldehydes, among others)[16a,19] have been performed, although most of the activation energies and Arrhenius preexponential factors have not been reported. According to the NIST chemical kinetics database,[4] before the second half of 1998 the activation energy of the NO_3 reaction with CH_3CHO was the only one determined. Rate constants have been reported for HCHO and CH_3CHO,[3a,b,c,20,21] but no kinetic data are available for FCHO and ClCHO. Furthermore, no previous theoretical determinations of the kinetic parameters for NO_3 reactions with aldehydes have been published.

The development of a reliable kinetic database for atmospheric reactions is of extreme importance. By knowing the

---

* To whom correspondence should be addressed. E-mail: boyd@is.dal.ca

[†] Permanent Address: Laboratorio de Química Computacional y Teórica. Facultad de Química, Universidad de La Habana, Habana 10400, Cuba.

10.1021/jp0125000 CCC: $22.00

activation energy and rate constant of every reaction taking place in the atmosphere, it would be possible to predict the chemical destiny of all compounds emitted to or generated in the atmosphere. This knowledge would also allow us to estimate the lifetime of every atmospheric species so that it would be possible to foresee their degree of migration into the different atmospheric regions, and their potential consequences. Unfortunately such experimental studies are often difficult to achieve and therefore theoretical predictions are an important alternative.

Due to the lack of kinetic information concerning the reaction of NO_3 with aldehydes, we decided to extend our previous studies[5] on the reactions with OH radicals to the NO_3 hydrogen-abstraction reactions with the same series of aldehydes (XCHO: X = F, Cl, H, CH_3): Previous calculations on the reaction of formaldehyde with OH[5a] showed why the addition reaction of OH to the carbonylic double bond does not occur. Since the NO_3 radical is less reactive than the OH radical we should not expect the addition reaction of NO_3 to be of any importance. Dluglokencky and Howard,[21b] confirmed an abstraction mechanism for the $CH_3CHO + NO_3$ reaction, on the basis of the nondetection of NO_2 in the product mixture and also because of the positive temperature dependence of the rate constant found.

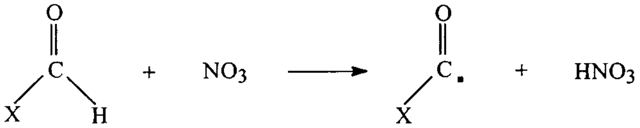

In the present study, high level ab initio calculations are performed to investigate the NO_3 hydrogen-abstraction reaction from FCHO, ClCHO, HCHO, and CH_3CHO. In addition, classical TST is applied to the calculation of the rate constants and tunneling corrections are considered. Our aim is to provide accurate theoretically determined kinetic parameters for these reactions.

Computational Details

Electronic structure calculations have been performed using the Gaussian 98 series of programs.[22] All geometries of the reactants, products and stationary points were fully optimized. Unrestricted ab initio methods were used to calculate the energy of the radical species. Geometries were optimized at the MP2(FC) and BH&HLYP[23] levels, and the character of all species was confirmed by a frequency calculation at the same level. Energies at the CCSD(T) level were calculated using the MP2 and BH&HLYP geometries, and in all cases the 6-311G(d,p) basis set was used.

In related papers,[5a] CCSD(T) energies obtained from MP2(FC) geometries using the 6-311++G(d,p) basis set, were sufficiently good to reproduce experimental activation energies and rate constants for the reaction of OH radicals with HCHO and CH_3CHO. A later study on the HCHO + OH system,[24] which contains a comparative discussion on the performance of different levels of theory (MP2, MP4, B3LYP, BH&HLYP), showed that the CCSD(T)//MP2(FC) selection of methods gives the best results for this system and that the inclusion of diffuse functions on the hydrogen atoms does not change the results significantly. BH&HLYP, combined with a CCSD(T) single point calculation, works better for this system than the other hybrid DFT methods we tried. CCSD(T)//B3LYP barriers are too low, resulting in rate constants larger than expected. In addition, we should mention that in previous studies[25] with DFT methods it was concluded that BH&HLYP is the best functional to characterize transition state (TS) structures, vibrational frequencies, and classical barrier heights for several reactions, including some hydrogen transfer processes. Furthermore, the addition of diffuse or polarization functions to the 6-311G(d,p) basis set has been shown to be unimportant.[25b] Therefore, for the NO_3 reactions we decided not to include diffuse functions in the basis set.

For reasons discussed below, the reactions were assumed to occur in a one-step mechanism:

$$XCHO + NO_3 \rightarrow XCO + HNO_3 \quad (X = F, Cl, H, CH_3)$$

According to classical TST, the expression to calculate the direct or elementary rate constants, k_D, can be written as

$$k_D = \kappa_D \frac{k_B T}{h} \frac{Q^{TS}}{Q^{react}} \exp\left(-\frac{(E^{TS} - E^{react})}{k_B T}\right) \tag{1}$$

where κ_D is the tunneling factor, k_B is Boltzmann's constant, h is Planck's constant, E^X and Q^X are total molecular energies (at 0 K) and standard molar partition functions (divided by Avogadro's number) of the TS and the reactants (react), respectively. These partition functions are approximated as products of electronic, vibrational, internal-rotational (where applicable), rotational, and translational partition functions.

Standard molar partition functions were calculated by using the molar volume of an ideal gas at the standard pressure (we have used p° = 1 atm) in the calculation of the translational partition function. Rotational constants and harmonic vibrational frequencies obtained from the ab initio calculations were used to calculate the rotational and vibrational components of the total partition function. For the TS, the contribution of the imaginary frequency to the vibrational partition function was excluded. This is the procedure followed by Gaussian 98.

The tunneling factor and the full width of the barrier at half its height ($\Delta s_{1/2}$) were calculated by assuming an unsymmetrical Eckart barrier.[8] The values of these two magnitudes depend on the forward and reverse energy barriers and also on the value of the imaginary frequency of the TS. A modified version of the numerical integration program of Brown[26] was used for the calculation of the tunneling factor, in which the numerical integration was performed over a 40-point Gaussian quadrature. Additional support for this model to estimate tunneling corrections is given elsewhere.[5b]

Results and Discussion

1. The NO_3 Radical. There is a great deal of conflicting evidence both experimental and theoretical as to the ground electronic state and geometry of NO_3.[15] While the experimental evidence[16b,27] suggests a D_{3h} equilibrium ground state, quantum chemical studies are divided between D_{3h}[28] and C_{2v}[29] (or even C_s), depending on the applied method. Two C_{2v} structures have been considered in the theoretical calculations and these have been previously denoted as 1L2S and 1S2L,[29b] according to the number of short (S) and long (L) NO bonds. Discrepancies between these predictions are partly due to the inherent difficulties of treating NO_3 properly, since it is an open-shell molecule with partial double bonds and low-lying excited electronic states.

Several coupled-cluster calculations of different types have led to contradictory results for the NO_3 ground state equilibrium geometry. A Fock space multireference CCSD (FSMR−CCSD) calculation yielded the symmetric D_{3h} structure as the global minimum on the potential surface,[28g,h] whereas a quasirestricted

TABLE 1: Calculations on the NO_3 Radical at Different Levels of Theory Using the 6-311G(d,p) Basis Set[a]

geometry	MP2(FC) D_{3h}	BH&HLYP D_{3h}	MP2(FC) C_{2v} '1S2L'	BH&HLYP C_{2v} '1S2L'	MP2(FC) C_{2v} '1L2S'	BH&HLYP C_{2v} '1L2S'
$d(N,O^1)$	1.244		1.181		1.380	
$d(N,O^2)$, $d(N,O^3)$	1.244		1.247		1.204	
$\angle(O^1,N,O^2)$	120.0		127.0		113.6	
E(PMP2)	−279.66345		−279.64122		−279.62950	
E(CCSD(T)//MP2(FC))	−279.66671		−279.66367		−279.66343	
NImag[b]	0		0		0	
$d(N,O^1)$		1.210		1.174		1.326
$d(N,O^2)$		1.210		1.241		1.184
$\angle(O^1,N,O^2)$		120.0		126.2		114.3
E(BH&HLYP)		−280.12240		−280.12821		−280.13238
E(CCSD(T)//BH&HLYP)		−279.66323		−279.66297		−279.66251
NImag[b]		2		1		0

[a] Atomic distances in Å, angles in degrees, and energies in au. [b] Number of imaginary frequencies.

Hartree−Fock CCSD (QHF−CCSD) calculation generated a C_{2v} (1L2S) ground state;[29c] the same result was obtained with Brueckner orbitals.[29a] In contrast, by including triple excitations in single-point calculations, the global minimum was found to be of D_{3h} symmetry.[28f]

A very interesting study on symmetry breaking and its effects on the potential surface of NO_3 was recently performed by Eisfeld and Morokuma.[28a] The authors refer to the symmetry breaking[30] of the electronic HF wave function as a problem frequently encountered in systems of high nuclear symmetry. The symmetry breaking or "symmetry dilemma", as named by Löwdin,[30] is an artifact caused by an inadequate approximate solution of the electronic Schrödinger equation. Apparently, this phenomenon results from a dominance of the orbital localization effect over the resonance effect and leads to three different solutions for the ground electronic state of NO_3, corresponding to equilibrium geometries that are not connected on the same potential energy surface. Eisfeld and Morokuma's study concludes that the effective equilibrium geometry of the NO_3 radical is D_{3h}. Their calculations, performed at the MR−SDCI level with selected electronic configurations and an N-electron basis of CASSCF orbitals, showed that even CCSD and CCSD(T) cannot completely overcome the symmetry breaking of the reference function and that three solutions with slightly different energies are obtained. Their study also confirmed previous observations[28f] about the inclusion of triplets in coupled-cluster calculations.

It has been shown that spin-unprojected Møller−Plesset perturbation theory calculations (MP2 and MP4) predict the NO_3 ground state to be of D_{3h} symmetry,[29b] although MP2 results still suffer from artifactual symmetry breaking since three different results are obtained.[28a]

In general, DFT methods have been reported to yield D_{3h} symmetric densities and equilibrium geometries for the NO_3 radical.[28c,e,29b] A study by Sherrill et al.[28c] showed that DFT methods tend to avoid artifactual spatial symmetry breaking in the equilibrium geometry region even when unrestricted Hartree−Fock (UHF) fails. They also showed that the exchange functional seems to be more important than the correlation functional in determining whether a symmetry-broken solution is obtained, and that hybrid functionals which include large amounts of HF exchange lead to symmetry breaking.

The results obtained for the NO_3 radical at the levels of calculation employed in this work are listed in Table 1. At the MP2 level the D_{3h} structure is the minimum, while at the BH&HLYP level the NO_3 molecule prefers a C_{2v} (1L2S) structure, the D_{3h} structure being a saddle point of second order. With both geometries, the CCSD(T) single point calculation predicts the D_{3h} structures to be of lower energy. Our calculations on the NO_3 radical are in agreement with the previous studies.

TABLE 2: Calculation of the Hydrogen Affinities (HA, in kJ/mol) of Some Radicals of Interest at the PMP2 level using MP2(FC)/6-311++D(d,p) Geometries

radical (X)	HA[a]
OH	−508.2
NO_3	−389.5
HCO	−368.1
CH_3CO	−371.8

[a] $HA_X = E_{HX} - (E_H + E_X)$.

The present study does not attempt to add new insight into the previous discussion about the NO_3 ground-state symmetry. The above controversy will be used later in the paper to justify our selection of computational methods.

By simple inspection of the reported activation energies and rate constants for the OH and NO_3 reactions from aldehydes,[4] it is easy to realize that NO_3 is a less reactive molecule. This situation can be justified by analyzing the spin density distribution in the radicals. In the D_{3h} NO_3 molecule, the spin density is homogeneously distributed among the oxygen atoms, while for the OH radical the spin density distribution is localized on oxygen. Another chemical reason to explain the smaller reactivity of the NO_3 radical can be found in its smaller hydrogen affinity, HA (see Table 2). The HA of NO_3 radicals is much smaller than that of OH, and not too much larger than the HA of HCO and CH_3CO, radicals with which the NO_3 radicals have to compete. As a result of the lower reactivity of NO_3 radicals, we should expect less stable reactant complexes and higher activation energies to form the TS, in comparison to the results obtained for the analogous OH−aldehyde reactions.[5]

2. The Reaction of NO_3 Radicals with HCHO and CH_3CHO. We begin by explaining our selection of the best combination of methods that reproduce the experimental kinetics of the NO_3 hydrogen-abstraction reaction from HCHO and CH_3CHO. The experimental rate constants, Arrhenius preexponential factors and activation energies are listed in Tables 3 ($CH_3CHO + NO_3$) and 4 ($HCHO + NO_3$).

Previous calculations on the OH reaction with CH_3CHO[5a] showed that the abstraction of the aldehydic hydrogen atom is favored. It has also been shown that the rate constant for the abstraction of one of the methyl hydrogen atoms is 10 times smaller.[3d] Since the NO_3 radicals are less reactive than the OH radicals, they should be more selective and the aldehydic hydrogen-abstraction should be the dominant process taking place in the reaction of NO_3 with CH_3CHO.

TABLE 3: Experimental Kinetic Results for the NO_3 Reaction with CH_3CHO

E_a[a]	A[b]	k[b]	T (K)	P (atm)	ref (year)
16.3		$1.58 \cdot 10^6$	263−363	1	21a (2001)
(15.46 ± 4.16)	8.43×10^8	1.64×10^6	260−370		3a (1999)[d]
15.5	8.43×10^8	1.64×10^6	260−370		3b (1997)[d]
(15.80 ± 2.53)	8.43×10^8	1.44×10^6	200−300		3c (1997)[d]
(15.49 ± 0.31)	$(8.67 \pm 0.87) \cdot 10^8$	1.67×10^6	264−374		20a (1991)[d]
(15.46 ± 2.47)	$(8.67 \pm 1.00) \cdot 10^8$	1.69×10^6	264−374	[c]	21b (1989)
		$(1.26 \pm 0.4) \times 10^6$	299	0.921	13a (1986)
		$(8.1 \pm 1.7) \times 10^5$	298	0.974	20d (1984)
		$(7.23 \pm 1.25) \times 10^5$	300	0.987	21c (1974)

[a] kJ/mol. [b] At 298 K, in L/mol·s. [c] 0.00132−0.00145 atm. [d] Literature review.

TABLE 4: Experimental Kinetic Results for the NO_3 Reaction with HCHO

E_a[a]	A[b]	k[b]	T (K)	P (atm)	ref (year)
20.2[e]	1.20×10^{9c}	3.49×10^5	298		3a (1999)[d]
		$(3.49 \pm 2.00) \times 10^5$	298		3b (1997)[d]
		3.49×0^5	298		3c (1997)[d]
		$(3.49 \pm 2.00) \times 10^5$	298		20a (1991)[d]
		$(3.25 \pm 0.65) \times 10^5$	295	0.974	20b (1988)
		$(3.79 \pm 0.64) \times 10^5$	298	0.921	20c (1985)
		$(1.95 \pm 0.16) \times 10^5$	298	0.974	20d (1984)

[a] kJ/mol. [b] At 298 K, in L/mol·s. [c] Suggested in ref. 3a (1999). [d] Literature review.

While this paper was in preparation, a publication by D'Anna and co-workers[21a] reported the rate coefficient of the acetaldehyde reaction with NO_3 by the absolute rate fast-flow-discharge technique and by a relative method. They also optimized the TS of the aldehydic and methyl hydrogen-abstraction reactions at the MP2/cc-pVDZ level, although activation energies were not estimated theoretically. Their experimental and theoretical results point to the aldehydic hydrogen-abstraction reaction as the only pathway for the NO_3 reaction with acetaldehyde under atmospheric conditions, in agreement with ideas derived from a previous work[16a] based on bond dissociation energies.

Energies obtained at different levels of theory were used to calculate the activation energy of the $CH_3CHO + NO_3$ reaction, and the values obtained are shown in Table 5, along with the calculated reaction enthalpies (both at 0 and 298.15 K). This is the only reaction among those studied for which activation energy values have been measured.

The PMP2 barrier is overestimated, as usual. This time the CCSD(T) calculation using MP2 geometries gives barriers that are still too high in comparison with experiment. The BH&HLYP and CCSD(T)//BH&HLYP barriers are too low. To correct these last two barriers, an estimate of the magnitude of the basis set superposition error (BSSE)[31] was calculated by applying the counterpoise (CP) method[32] to the TS, following the original procedure in which the "monomeric units" (the reactants) upon forming the "intermolecular complex" (the TS) are not further optimized, i.e., the "monomers" are frozen in their supermolecular geometries.

Estimates of the effects of the BSSE by the CP method have been found to be misleading for hydrogen bonded dimers, since they do not provide quantitative information about the basis set deficiencies.[33] Furthermore, it has been shown that the use of large enough basis sets so that the CP correction is small does not guarantee accurate results and that for smaller basis sets the inclusion of this correction does not systematically improve the accuracy of the calculations.[34] Despite these criticisms and the fact that other methods for correcting the BSSE have been discussed in the literature,[35] the CP correction continues to be most widely used method for this purpose.[36]

The BSSE was calculated using BH&HLYP as well as CCSD(T) (only for the $CH_3CHO-NO_3$ TS) energies, and are denoted BSSE(BH&H) and BSSE(CC), respectively. When these two corrections are added to the CCSD(T)//BH&HLYP barrier, activation energies in good agreement with experiment are obtained.

Bearing in mind the uncertainty about the ground-state symmetry of the NO_3 radical, we decided to try another correction to the CCSD(T)//BH&HLYP barrier. Since the lowest CCSD(T) energy for NO_3 is obtained at the MP2(FC)-D_{3h} geometry (see Table 1), we choose to combine this result with the previous CCSD(T)//BH&HLYP calculations. That is, BH&HLYP geometries are used in the single point CCSD(T) calculations except for NO_3 for which the MP2(FC)-D_{3h} structure is used. Frequency calculations are performed at the BH&HLYP level. Results using this correction will be denoted CCSD(T)//BH&HLYP(MP2) throughout the text. The activation energy obtained (16.3 at 0 K and 18.5 at 298 K, in kJ/mol) is in very good agreement with experiment (15.5−16.3 kJ/mol). The reaction enthalpy calculated in this way is −53.6 at 0 K, and −53.3 at 298 K (in kJ/mol), also in very good agreement with the latest experimental value (−53.3 kJ/mol).

For the HCHO + NO_3 reaction the calculated activation energies and reaction enthalpies have been reported in Table 6 (both at 0 and 298 K). For this reaction an activation energy of 20.2 kJ/mol has been suggested by analogy with the reaction of NO_3 with CH_3CHO.[3a] The best results are once again obtained at the CCSD(T)//BH&HLYP level after considering the above-mentioned corrections (CCSD(T)//BH&HLYP + BSSE(BH&H) and CCSD(T)//BH&HLYP (MP2)). The reaction enthalpy obtained at the CCSD(T)//BH&HLYP(MP2) level (−59.1 kJ/mol) is in excellent agreement with experiment as well (−57.1 kJ/mol).

The values of the partition functions needed for the calculation of the TST rate constants of the reactions studied at MP2 and BH&HLYP levels of theory are given in Table 7, as well as the imaginary frequency of the TS. Several low frequencies (below 300 cm^{-1}) in addition to the imaginary frequency were calculated for the hydrogen-abstraction TS. Of these, three were identified as internal rotations (or torsional vibrations) by visualization of the normal modes. These harmonic modes correspond most closely to the three new internal rotors created in the TS ($XCOH\cdots ONO_2$, $XCO\cdots HNO_3$, and $XCOHO\cdots NO_2$), where the common axes for internal rotation are the ones linking the reactants, products, and one along the N−O bond with the oxygen atom abstracting the hydrogen. These were the axes considered in the calculation of the reduced moments of inertia. These harmonic modes were treated as free rotors in the calculation of the internal rotation partition function of the TS (Q_{IR}^{TS}).[37,38] This has also been the procedure followed in previous related studies.[5,39]

The harmonic contributions of these low frequencies were eliminated from the vibrational partition function in order to

TABLE 5: Activation Energy (E_a) and Reaction Enthalpy (ΔH), in kJ/mol at 0 and 298.15 K, for the NO_3 Hydrogen-Abstraction Reaction from CH_3CHO at Different Levels of Theory

basis set: 6-311G(d,p)	$E_a^{(0\ K)}$	$E_a^{(298\ K)}$	$\Delta H^{(0\ K)}$	$\Delta H^{(298\ K)}$
PMP2	109.7	111.7	−32.4	−31.1
CCSD(T)//MP2(FC)	23.2	25.3	−75.6	−74.3
BH&HLYP	−0.3	1.9	−65.5	−65.1
CCSD(T)//BH&HLYP	5.3	7.5	−64.7	−64.3
BH&HLYP + BSSE(BH&H)	6.9	9.1		
CCSD(T)//BH&HLYP + BSSE(BH&H)	12.4	14.6		
CCSD(T)//BH&HLYP + BSSE(CC)	18.8	21.0		
CCSD(T)//BH&HLYP(MP2)	16.3	18.5	−53.6	−53.3
experiment		16.3[a]		−53.3[d]
		(15.46 ± 4.16)[b]		−67.3[e]
		(15.80 ± 2.53)[c]		

[a] Ref. 21a (2001). [b] Ref. 3a (1999), 3b (1997), 20a (1991), 21b (1989). [c] Ref. 3c (1997). [d] Ref. 3a (1999). [e] Ref. 3b (1997).

TABLE 6: Activation Energy (E_a) and Reaction Enthalpy (ΔH), in kJ/mol, at 0 and 298.15 K for the NO_3 Hydrogen-Abstraction Reaction from HCHO at Different Levels of Theory

basis set 6-311G(d,p)	$E_a^{(0\ K)}$	$E_a^{(298\ K)}$	$E_{a(-1)}^{(0\ K)}$	$E_{a(2)}^{(298\ K)}$	$\Delta H^{(0\ K)}$	$\Delta H^{(298\ K)}$
PMP2	118.2	119.3	−70.0	48.2	−41.2	−40.2
CCSD(T)//MP2(FC)	32.4	33.6	10.7	43.2	−81.1	−80.1
BH&HLYP	3.2	3.9	5.1	8.3	−70.1	−70.0
CCSD(T)//BH&HLYP	11.3	12.0	6.7	18.0	−70.3	−70.2
BH&HLYP + BSSE(BH&H)	10.2	10.9				
CCSD(T)//BH&HLYP + BSSE(BH&H)	18.3	19.0				
CCSD(T)//BH&HLYP*	22.4	23.1	−4.4	18.0	−59.3	−59.1
experiment		20.2[a]				−57.1[b]
						−58.4[c]

[a] Suggested in ref. 3a (1999), 3b (1997). [b] Ref. 3a (1999). [c] Ref. 3b (1997).

TABLE 7: Total Partition Functions (Q) of the Reactants and the TS, and Imaginary Frequency ($\nu^{\ddagger}$ in cm^{-1}) of the TS of the NO_3 Hydrogen-Abstraction Reaction from XCHO (X = F, Cl, H, CH_3), Calculated at Different Levels of Theory

level of theory	calculation	FCHO + NO_3	ClCHO + NO_3	HCHO + NO_3	CH_3CHO + NO_3
MP2(FC)/6-311G(d,p)	$Q^{NO_3}{}_{(D_{3h})}$	1.70737×10^{11}	1.70737×10^{11}	1.70737×10^{11}	1.70737×10^{11}
	Q^{XCHO}	1.13573×10^{11}	3.90682×10^{11}	4.61479×10^{9}	2.97963×10^{11}[a]
	Q^{TS}	3.90874×10^{15}	1.44419×10^{16}	7.39244×10^{14}	1.53333×10^{16}
	$\prod Q_{\nu=i}$[f]	28.649[b]	41.307[c]	17.383[d]	90.815[e]
	$Q_{IR}{}^{TS}$[g]	4.78689×10^{4}	8.51824×10^{4}	1.55481×10^{4}	1.64320×10^{5}
	$Q_{corr}{}^{TS}$[h]	6.53102×10^{18}	2.97821×10^{19}	6.61219×10^{17}	2.77441×10^{19}
	$\nu^{\neq}$	2703	2335	1395	998
BH&HLYP/6-311G(d,p)	$Q^{NO_3}{}_{(C_{3v})}$	5.50530×10^{11}	5.50530×10^{11}	5.50530×10^{11}	5.50530×10^{11}
	Q^{XCHO}	1.08003×10^{11}	3.79813×10^{11}	4.42745×10^{9}	2.79523×10^{11}[i]
	Q^{TS}	5.34208×10^{15}	1.82529×10^{16}	1.09900×10^{15}	8.36021×10^{16}
	$\prod Q_{\nu=i}$[f]	33.585[j]	48.383[k]	23.921[l]	393.66[m]
	$Q_{IR}{}^{TS}$[g]	4.68184×10^{4}	8.46634×10^{4}	1.38936×10^{4}	1.66813×10^{5}
	$Q_{corr}{}^{TS}$[h]	7.44708×10^{18}	3.19401×10^{19}	6.38324×10^{17}	3.54265×10^{19}
	$\nu^{\neq}$	1983	1503	239	141

[a] $Q_{corr}{}^{CH_3CHO} = 5.39632 \times 10^{11}$. [b] $i = 1, 3, 4$. [c] $i = 1, 3, 4$. [d] $i = 1, 2, 4$. [e] $i = 1, 2, 4, 6$. [f] Vibrational components that were eliminated from the calculation of $Q_{corr}{}^{TS}$. [g] Total internal-rotational partition function of the TS. [h] Corrected total partition function of the TS. [i] $Q_{corr}{}^{CH_3CHO} = 5.10774 \times 1011$. [j] $i = 1, 3, 4$. [k] $i = 1, 3, 4$. [l] $i = 1, 2, 4$. [m] $i = 1, 2, 4, 6$.

correct the total partition function of the TS ($Q_{corr}{}^{TS}$):

$$Q_{corr}{}^{TS} = \frac{Q^{TS} Q_{IR}{}^{TS}}{\prod Q_{\nu=i}}$$

For CH_3CHO and its TS, the internal rotation around the C−C single bond was also considered and treated as a free rotor.

TST direct (elementary) rate constants (k_D) at 298 K for the reactions of CH_3CHO and HCHO with NO_3 radicals calculated at different levels of theory are given in Tables 8 and 9, respectively. Some experimental results have been included for comparison. The tunneling corrections (κ) have also been reported in these tables.

In both cases the CCSD(T)//BH&HLYP(MP2) calculation gives the best rate constants (1.11×10^6 for $CH_3CHO + NO_3$ and 2.09×10^5 for $HCHO + NO_3$), in very good agreement with experiment ($1.26-1.69 \times 10^6$ for $CH_3CHO + NO_3$ and $1.95-3.79 \times 10^5$ for $HCHO + NO_3$). Rate constants at other levels of calculation are not able to reproduce the order of the experimental values for both reactions. The CCSD(T)//MP2(FC) rate constants are less than an order below experiments but the activation energies for both reactions are overestimated. From this we conclude that the CCSD(T)//BH&HLYP(MP2) should be the best method to predict the unknown kinetic parameters.

2.1. Elementary or Complex Reactions? The significance of considering the complex character of the kinetics of a radical−molecule reaction was one of the main conclusions of a recent publication.[5a] Later it was shown that even for reactions with less stable reactant complexes and higher activation energies (FCHO + OH and ClCHO + OH)[5b] a complex mechanism should also be considered. Furthermore, it was shown that for

TABLE 8: Rate Constants (k_D in L/mol·s) and Tunneling Corrections (κ_D) for the NO_3 Hydrogen-Abstraction Reaction from CH_3CHO, Calculated at Different Levels of Theory Using the 6-311G(d,p) Basis Set and Considering a Direct Mechanism at 298.15 K

level of calculation	κ_D	k_D	ref (year)
PMP2	3.33	3.82×10^{-10}	
CCSD(T)//MP2(FC)	2.81	4.45×10^{5}	
BH&HLYP	–	8.69×10^{8}	
CCSD(T)//BH&HLYP	1.02	9.51×10^{7}	
BH&HLYP + BSSE(BH&H)	1.02	4.95×10^{7}	
CCSD(T)//BH&HLYP + BSSE(BH&H)	1.02	5.31×10^{6}	
CCSD(T)//BH&HLYP + BSSE(CC)	1.02	4.10×10^{5}	
CCSD(T)//BH&HLYP(MP2)	1.02	1.11×10^{6}	
experiment		1.58×10^{6}	21a (2001)
		1.64×10^{6}	3a (1999), 3b (1997)
		1.44×10^{6}	3c (1997)
		1.67×10^{6}	20a (1991)
		1.69×10^{6}	21b (1989)
		$(1.26 \pm 0.24) \times 10^{6}$	13a (1986)

TABLE 9: Rate Constants (k_D in L/mol·s) and Tunneling Corrections (κ_D) for the NO_3 Hydrogen-Abstraction Reaction from HCHO, Calculated at Different Levels of Theory Using the 6-311G(d,p) Basis Set for the Direct and Complex Mechanisms at 298.15 K

	direct mechanism		complex mechanism		
level of calculation	κ_D	k_D	κ	k_{eff}	ref (year)
PMP2	23.16	2.39×10^{-10}	11.97	1.24×10^{-10}	
CCSD(T)//MP2(FC)	8.96	9.66×10^{4}	11.08	1.19×10^{5}	
BH&HLYP	1.05	4.78×10^{8}	1.06	4.81×10^{8}	
CCSD(T)//BH&HLYP	1.06	1.78×10^{7}	1.06	1.78×10^{7}	
BH&HLYP + BSSE(BH&H)	1.06	2.86×10^{7}	1.06	2.86×10^{7}	
CCSD(T)//BH&HLYP + BSSE(BH&H)	1.06	1.06×10^{6}	1.06	1.06×10^{6}	
CCSD(T)//BH&HLYP(MP2)	1.06	2.09×10^{5}	1.06	2.08×10^{5}	
experiment		$(3.49 \pm 2.00) \times 10^{5}$			3a (1999), 3b, 3c (1997), 20a (1991)
		$(3.25 \pm 0.65) \times 10^{5}$			20b (1988)
		$(3.79 \pm 0.64) \times 10^{5}$			20c (1985)
		$(1.95 \pm 0.16) \times 10^{5}$			20d (1984)

these two reactions, the percent difference between the elementary (direct) and complex (effective) rate constants was smaller than the difference found for the HCHO + OH reaction, in which a smaller activation energy was found. It was rationalized that the larger the effective energy barrier for radical−molecule reactions and the smaller the stabilization energy of the reactant complex, the more closely its behavior resembles an elementary reaction.

Intuitively for the NO_3 reactions we should expect higher activation energies and less stable reactant complexes, and then a smaller percent difference between the elementary and complex rate constants in comparison with the analogous OH reactions. In other words, the kinetic behavior of the NO_3 reactions should resemble more closely a bimolecular elementary reaction, and we would like to determine whether the assumption of considering these reactions to be elementary is valid or if we need to consider the formation of the reactant complex.

For the simplest system, the HCHO + NO_3 reaction, two possible mechanisms were considered: a direct or one-step mechanism, in which the hydrogen abstraction takes place in an elementary step, and a two-step mechanism that involves a fast preequilibrium between the reactants and the reactant complex (RC), followed by the irreversible hydrogen abstraction that takes place in the reactant complex to form the products (product complex):

$$\text{Step 1:}\quad HCHO + NO_3 \rightleftarrows [HCHO\cdots NO_3]$$

$$\text{Step 2:}\quad [HCHO\cdots NO_3] \rightarrow [HCO\cdots HNO_3]$$

$$\text{Step 3:}\quad [HCO\cdots HNO_3] \rightarrow HCO + HNO_3$$

The overall rate constant for the formation of the product complex following the above complex mechanism (k_{eff}) can be written as

$$k_{eff} = \frac{k_1 k_2}{k_{-1}} = K_{eq} k_2$$

where k_1 and k_{-1} are the forward and reverse rate constants, respectively, for the first step, and k_2 is the rate coefficient of the second step.

Applying basic statistical thermodynamics principles[41] for the calculation of the equilibrium constant of the first step (K_{eq}) and the classical TST formula to calculate k_2:

$$K_{eq} = \frac{Q^{RC}}{Q^{react}} \exp\left(-\frac{E^{RC} - E^{react}}{k_B T}\right)$$

$$k_2 = \kappa \frac{k_B T}{h} \frac{Q^{TS}}{Q^{RC}} \exp\left(-\frac{E^{TS} - E^{RC}}{k_B T}\right)$$

k_{eff} can be written as

$$k_{eff} = \kappa \frac{k_B T}{h} \frac{Q^{TS}}{Q^{react}} \exp\left(-\frac{(E^{TS} - E^{react})}{k_B T}\right) \tag{2}$$

The only difference between expressions 1 and 2 lies in the value of the tunneling factor, which depends on the forward and reverse potential energy barriers of the elementary process in which the hydrogen atom is abstracted. For the complex mechanism these energy barriers are calculated from the energies (including ZPC) of the reactant complex, TS, and product

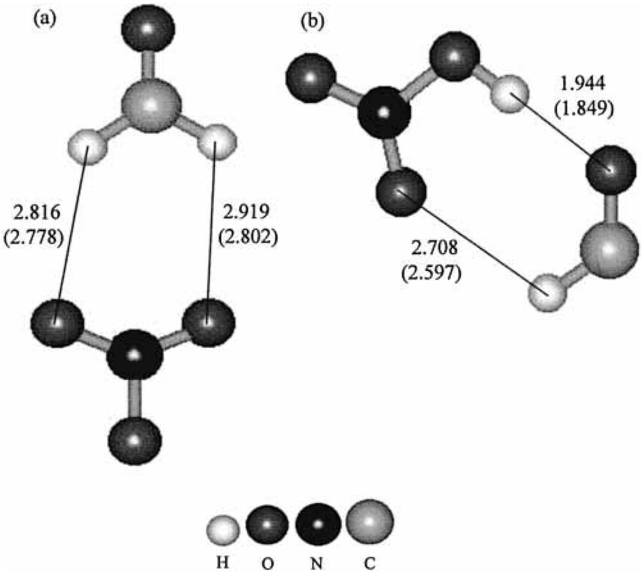

Figure 1. Optimized structures of the (a) reactant and (b) product complexes in the HCHO + NO_3 hydrogen-abstraction reaction, as obtained at the MP2(FC) (BH&HLYP) level with the 6-311G(d,p) basis set.

complex, while for the direct mechanism the energies of the isolated reactants and products as well as the energy of the TS are the ones to be considered. The geometry of the reactant and product complexes of the HCHO + NO_3 reaction are shown in Figure 1, where some geometrical parameters have been indicated.

The stabilization energy of the reactant complex ($E_{a\,(-1)}$) and the activation barrier of the second step of the complex mechanism ($E_{a(2)}$) at 0 K, are given in Table 6. At the CCSD(T)//MP2(FC) level the reactant complex was found to be 10.7 kJ/mol lower in energy than the isolated reactants. At this level, but using a slightly larger basis set, 6-311++G(d,p), the stabilization energy of the reactant complex for the HCHO + OH reaction was calculated to be 13.6 kJ/mol. The new complex is less stable, as expected. At the CCSD(T)//BH&HLYP level this energy was 6.7 kJ/mol. Since as shown before in Tables 5 and 6, CCSD(T)//MP2 and CCSD(T)/BH&HLYP energy differences are overestimated and underestimated, respectively, we should expect a more realistic value of the reactant complex stabilization energy between the values calculated at these two levels (6.7 and 10.7 kJ/mol). The calculated reaction profiles for the HCHO + NO_3 reaction at different levels of theory are shown in Figure S1 of the Supporting Information.

Rate constants calculated for the direct and complex mechanisms are reported in Table 9. At the CCSD(T)//MP2 level the difference is small. The percentage by which these two rate constants differ, calculated by

$$\left(\frac{k_{\mathrm{eff}} - k_{\mathrm{D}}}{k_{\mathrm{eff}}}\right) \times 100\%$$

is 18.8%. For the OH hydrogen-abstraction reaction from the same series of aldehydes, this percent difference was calculated to be 71.3% for the FCHO reaction, the one with the highest activation energy and the least stable reactant complex. For the other calculations on the NO_3 reactions the difference between rate constants for the mechanisms considered is negligible. Hence, the assumption of an elementary mechanism for the NO_3 hydrogen-abstraction reaction from these aldehydes is valid.

3. Results and Discussions

The optimized geometries of the TSs of these reactions are shown in Figure 2, where relevant geometrical parameters have been indicated for the MP2 and BH&HLYP optimizations. The overall shape of these molecular systems did not change significantly at these two levels. The reaction profiles at the CCSD(T)/BH&HLYP(MP2) level of calculation are shown in Figure 3.

Cartesian coordinates of the stationary points optimized at MP2 and BH&HLYP levels are given as Supporting Information. The calculated total energies (PMP2, CCSD(T)//MP2, BH&HLYP, and CCSD(T)//BH&HLYP), zero-point and thermal (at 298.15 K) vibrational energy corrections (calculated at MP2 and BH&HLYP levels) of the species involved in the reaction of NO_3 with the aldehydes, and the BSSE calculated for the TS for these reactions are given as Supporting Information as well.

The symmetry of the TS calculated for the NO_3 reaction with HCHO and CH_3CHO is ${}^2A'$, (C_s point group), implying that the unpaired electron is in the plane where the NO_3 attack takes place. ${}^2A'$ is also the symmetry of the XCO radical generated. This corresponds to the TS structures obtained for the OH reactions.[5] However, for the FCHO and ClCHO hydrogen-abstraction reactions, the TSs possess C_1 symmetry. The oxygen atoms of the NO_3 radical avoid spatial interaction with the electronic cloud of the halogen atom of these aldehydes, and the best way of achieving this, without creating new destabilizing interactions, is by breaking the plane of symmetry. For HCHO and CH_3CHO, the distances between the closest oxygen atom (of the two not directly implied in the abstraction process) of the NO_3 to the nearest H of the aldehyde are 2.605 and 2.931 Å, respectively. Hydrogen bonding interactions stabilize these structures. For FCHO and ClCHO, the distances from the halogen atom to the closest O atom of NO_3 are 3.172 and 3.611 Å, respectively. The larger the halogen atom the greater this interatomic distance.

The structure of the TS of the CH_3CHO reaction reported in the work by D'Anna and co-workers,[21a] calculated at the MP2/cc-pVDZ level of theory, agrees to within 0.01 Å with our MP2 results.

In the series of substituents, F, Cl, H, and CH_3, the TS becomes more reactant-like (Figure 2). Thus, the C$\cdots$H distance decreases in this order from 1.195 Å (FCHO) to 1.160 (CH_3CHO) at the MP2 level and from 1.240 to 1.132 Å at the BH&HLYP level; in a similar way the H$\cdots$O distance gets enlarged. Furthermore, a larger activation energy has to be overcome. This trend is consistent with the decreasing electron-donating effect of these substituents that is also the cause of the decreasing reactivity of these aldehydes toward the NO_3 hydrogen-abstraction reaction. Similar results were discussed for the analogous OH reactions.[5b]

In the previously mentioned series of substituents (F, Cl, H, CH_3), the imaginary frequency of the TS ($\nu^{\ddagger}$) decreases at both levels of theory, and thus the curvature of the calculated barrier is reduced as well. The full width of the barrier at half its height ($\Delta s_{1/2}$) increases in the same order. In this series of aldehydes the tunneling factor (κ) decreases in agreement with the fact that activation energies and imaginary frequencies decrease. At the MP2 and BH&HLYP levels of theory barriers are predicted to reduce in height and curvature when going from FCHO to CH_3CHO. This was also the case for the OH hydrogen-abstraction reactions.[5]

As observed in many other situations, barriers calculated using BH&HLYP geometries are predicted to be smaller and wider

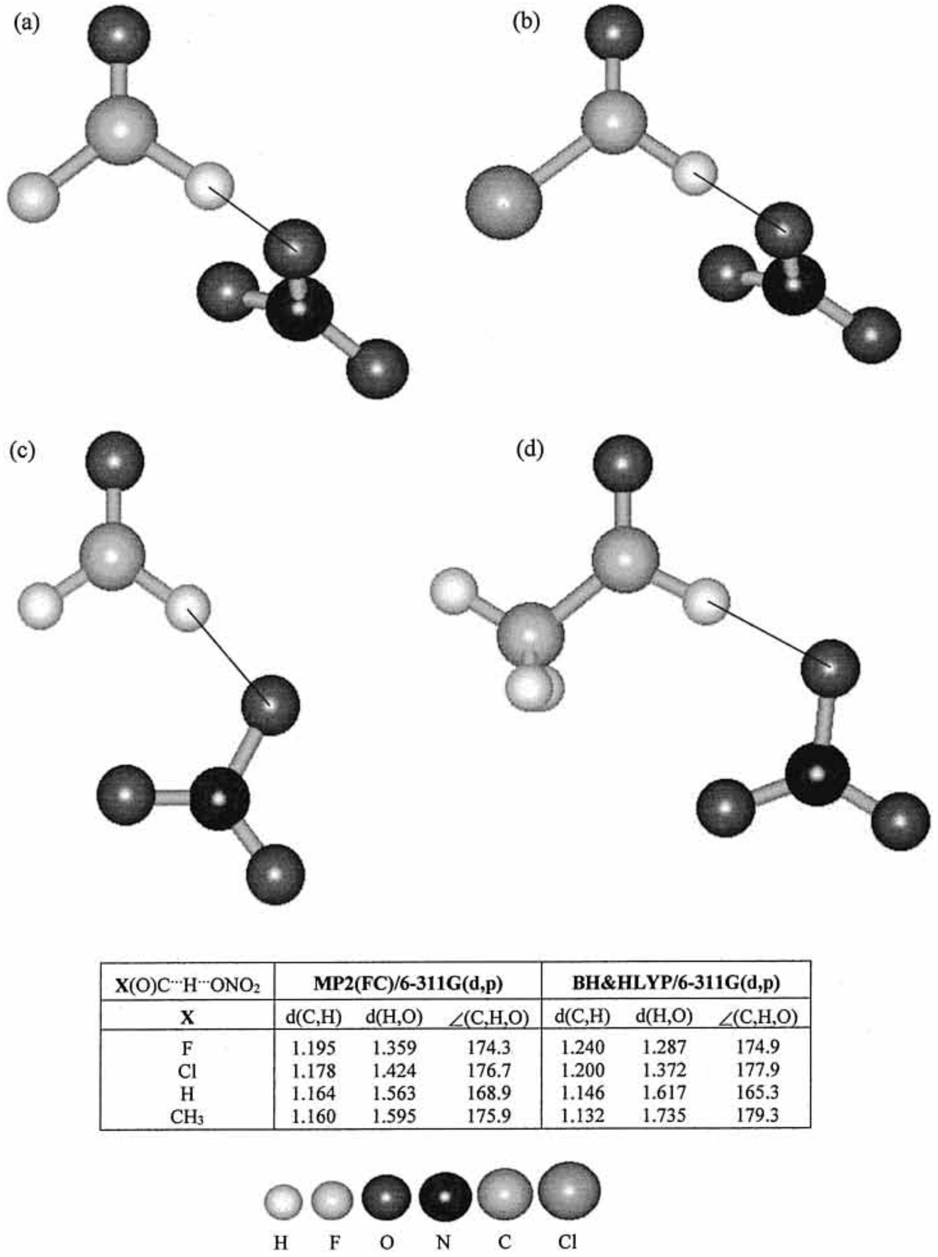

$X(O)C\cdots H\cdots ONO_2$	MP2(FC)/6-311G(d,p)			BH&HLYP/6-311G(d,p)		
X	d(C,H)	d(H,O)	∠(C,H,O)	d(C,H)	d(H,O)	∠(C,H,O)
F	1.195	1.359	174.3	1.240	1.287	174.9
Cl	1.178	1.424	176.7	1.200	1.372	177.9
H	1.164	1.563	168.9	1.146	1.617	165.3
CH_3	1.160	1.595	175.9	1.132	1.735	179.3

Figure 2. Structure of the transition states of the hydrogen-abstraction reactions studied and some relevant geometrical parameters. (a) FCHO + NO_3, (b) ClCHO + NO_3, (c) HCHO + NO_3, (d) CH_3CHO + NO_3.

than barriers calculated with MP2 structures. Tunneling corrections for BH&HLYP geometries are significantly smaller than the values calculated with MP2 structures, since barriers and imaginary frequencies are smaller too.

The predicted values of the activation energies and rate constants for the NO_3 hydrogen-abstraction reactions from FCHO and ClCHO, at 298K, calculated at the CCSD(T)//BH&HLYP(MP2) level are 60.2 kJ/mol and 10.30 L/mol·s for FCHO, and 37.0 kJ/mol and 9.01×10^8 L/mol·s for ClCHO. Reaction enthalpies are calculated to be −6.4 (FCHO) and −47.1 kJ/mol (ClCHO). These values, as well as activation energies and reaction enthalpies at 0 K and tunneling corrections calculated at different levels of theory, are shown in Tables 10 and 11. The calculated partition functions and imaginary frequency of the TS at MP2 and BH&HLYP levels are given in Table 7.

To obtain the CCSD(T) energy differences reported in Tables 5, 6, and 10, vibrational corrections at the level at which the geometries were optimized, MP2 or BH&HLYP, are used. For these reactions spin contamination at the TS is small; the highest expectation value of S^2 is 0.806 for the FCHO reaction at the MP2 level. Spin contamination is completely eliminated by projection at MP2 and BH&HLYP levels, hence CCSD(T) calculations could be considered reliable in this sense.

Tunneling corrections for the HCHO and CH_3CHO reactions with NO_3 radicals with geometries calculated at the BH&HLYP level are almost negligible (1.06 and 1.02, respectively). Hence we should expect an Arrhenius behavior for these reactions at temperatures above T^*, the characteristic tunneling temperature below which tunneling is significant. $T^*$is equal to $hc\nu^{\ddagger}/(2\pi k_B)$ and for the HCHO and CH_3CHO reactions is 55 and 32 K, respectively. Hence we should be able to calculate classical Arrhenius parameters for these reactions for temperatures above $T^*$by using the following well-known expression:

$$A = \frac{k_B T}{h} \frac{Q^{TS}}{Q^{react}}$$

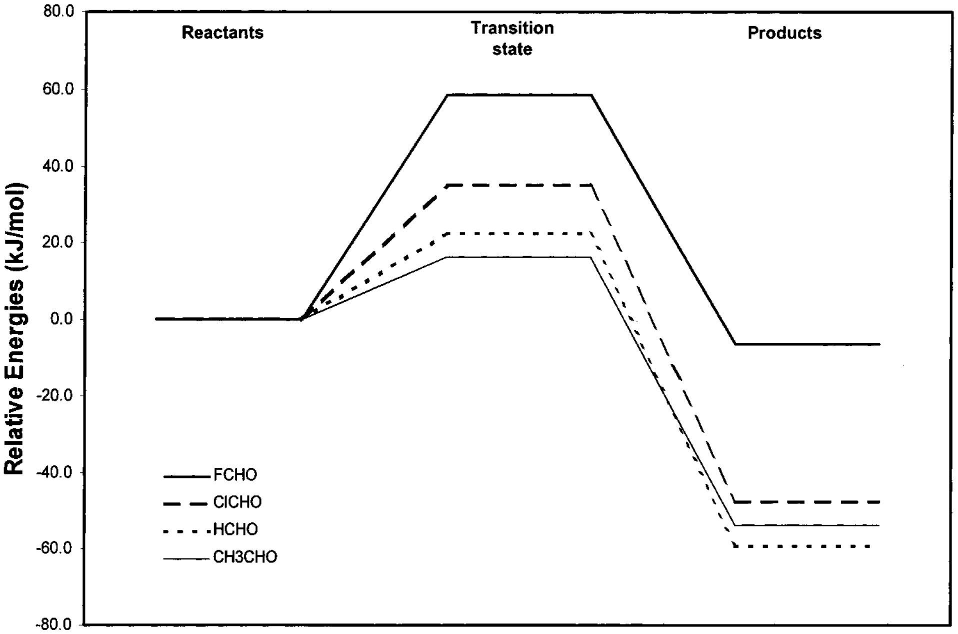

Figure 3. Reaction profile for the XCHO + NO_3 (X = F, Cl, H, CH_3) hydrogen-abstraction reactions using the calculated CCSD(T)/6-311G-(d,p)//BH&HLYP/6-311G(d,p) energy values, including the BH&HLYP/6-311G(d,p) zero-point energy corrections. Note: For the CCSD(T) calculation on the NO_3 radical, the MP2(FC)-D_{3h} geometry was the one employed.

TABLE 10: Activation Energy (E_a) and Reaction Enthalpy (ΔH), in kJ/mol, at 0 and 298.15 K, for the NO_3 Hydrogen-Abstraction Reaction from XCHO (X = F, Cl) at Different Levels of Theory Using Basis Set 6-311G(d,p)

	$E_a^{(0\ K)}$	$E_a^{(298\ K)}$	$\Delta H^{(0\ K)}$	$\Delta H^{(298\ K)}$
FCHO + NO_3				
PMP2	147.8	149.6	15.9	16.8
CCSD(T)//MP2(FC)	74.4	76.3	−28.2	−27.3
BH&HLYP	49.3	51.0	−13.4	−13.3
CCSD(T)//BH&HLYP	47.6	49.2	−17.5	−17.4
BH&HLYP + BSSE(BH&H)	58.5	60.1		
CCSD(T)//BH&HLYP + BSSE(BH&H)	56.7	58.4		
CCSD(T)//BH&HLYP(MP2)	58.6	60.2	−6.5	−6.4
ClCHO + NO_3				
PMP2	131.5	133.7	−25.1	−23.9
CCSD(T)//MP2(FC)	52.5	54.7	−68.7	−67.5
BH&HLYP	28.1	30.0	−55.5	−54.8
CCSD(T)//BH&HLYP	24.2	26.0	−58.8	−58.2
BH&HLYP + BSSE(BH&H)	37.3	39.1		
CCSD(T)//BH&HLYP + BSSE(BH&H)	33.3	35.2		
CCSD(T)//BH&HLYP*	35.2	37.0	−47.8	−47.1

TABLE 11: Rate Constants (k_D in L/mol·s) and Tunneling Parameters (κ_D) for the NO_3 Hydrogen-Abstraction Reaction from FCHO and ClCHO, Calculated at Different Levels of Theory Using the 6-311G(d,p) Basis Set and Considering a Direct Mechanism, at 298.15 K

	FCHO + NO_3		ClCHO + NO_3	
level of calculation	κ_D	k_D	κ_D	k_D
PMP2	4.53×10^7	1.23×10^{-9}	1.11×10^6	2.80×10^{-8}
CCSD(T)//MP2(FC)	8.05×10^4	15.55	1.34×10^3	2.36×10^3
BH&HLYP	162.25	2.85×10^2	11.19	1.25×10^5
CCSD(T)//BH&HLYP	152.76	5.49×10^2	9.66	5.34×10^5
BH&HLYP + BSSE(BH&H)	273.18	11.92	14.76	4.11×10^3
CCSD(T)//BH&HLYP + BSSE(BH&H)	260.34	23.42	13.19	1.81×10^4
CCSD(T)//BH&HLYP(MP2)	244.78	10.30	13.95	9.01×10^3

For CH_3CHO + NO_3 the preexponential factor (at 298 K, in units of L/mol·s) is calculated to be 7.83×10^8, in very good agreement with the experimental value ($8.43-8.67 \times 10^8$, see Table 3). For the HCHO + NO_3 reaction we predict the Arrhenius parameter to be 1.63×10^9, basically twice the A value for the CH_3CHO reaction, as expected since in HCHO there are two equivalent sites of attack. The suggested value[3a] of 1.20×10^9 at 298 K, based on the experimental results for the CH_3CHO + NO_3 reaction, is in agreement with our calculation.

For the FCHO and ClCHO reactions tunneling is significant. The calculated characteristic temperatures (T^*) are 454 and 344 K, respectively. Calculations of Arrhenius parameters using the above expression and ignoring tunneling quantum effects would be erroneous. If we include the value of κ in the above expression, the values of A for the FCHO and ClCHO reactions would be 1.90×10^{11} and 1.32×10^{10}, respectively. Although this is not the most appropriate way of estimating the quantum Arrhenius parameter, these values could be used as a reference when better determinations are made.

Conclusions

The NO_3 hydrogen-abstraction reaction from a series of aldehydes (XCHO: X = F, Cl, H, CH_3) has been studied by means of ab initio calculations. Optimizations at the MP2 and BH&HLYP levels followed by CCSD(T) single point calculations were performed using the 6-311G(d,p) basis set. Neither CCSD(T)//MP2 nor CCSD(T)//BH&HLYP calculations were successful in reproducing the kinetic and thermochemical data available for such reactions. Hence several corrections were considered to improve upon the CCSD(T)//BH&HLYP results, which were the closest to experiment. The use of the MP2-D_{3h} geometry of the NO_3 radical (for which a lot of controversial results regarding its ground state symmetry have been published) in the CCSD(T) calculation allowed us to reproduce the only six parameters for which experimental results exist: rate constants and reaction enthalpies for the CH_3CHO and HCHO reactions, and activation energy and Arrhenius preexponential factors for the CH_3CHO reaction with NO_3 radicals. At this level of theory the unknown values of rate constants, activation energies, and Arrhenius factors were then predicted theoretically for the first time, since no previous theoretical studies have been reported for the reactions between aldehydes and NO_3 radicals.

Furthermore, it was shown that these reactions can be considered elementary. The consideration of a reactant complex as in previous studies[5] does not affect the calculated kinetic results at the chosen level of theory. These results complement a series of studies regarding radical−molecule reactions and prove that even though for some reactions with low or negative activation energies the formation of the reactant complex needs to be considered, another extreme case, such as the NO_3 reactions studied, can be found for which a one-step mechanism is a good enough approximation for kinetic determinations.[5b]

Acknowledgment. The authors thank the Natural Sciences and Engineering Research Council of Canada (NSERC) for financial support. N.M.D. thanks Dalhousie University for a Graduate Scholarship.

Supporting Information Available: The calculated reaction profiles for the HCHO + NO_3 reaction at different levels of theory (Figure S1), as well as the MP2(FC)/6-311G(d,p) and BH&HLYP/6-311G(d,p) optimized geometries in Cartesian coordinates (Tables S1 to S4), total energies, zero-point and thermal (at 298.15 K) vibrational corrections, in atomic units, (Tables S5 and S6) of the species involved in the reactions studied, and the estimated BSSE for the TS. This information is available free of charge via the Internet at http://pubs.acs.org.

References and Notes

(1) Finlayson-Pitts, B. J.; Pitts, J. N. *Atmospheric Chemistry: Fundamentals and Experimental Techniques*, Wiley-Interscience: New York, 1986.

(2) Seinfeld, J. H.; Pandis, S. N. *Atmospheric Chemistry and Physics: From Air Pollution to Climate Change*, Wiley-Interscience: New York, 1998.

(3) (a) Atkinson, R.; Baulch, D. L.; Cox, R. A.; Hampson, R. F., Jr.; Kerr, J. A.; Rossi, M. J.; Troe, J. *J. Phys. Chem. Ref. Data* **1999**, *28*, 191. (b) Atkinson, R.; Baulch, D. L.; Cox, R. A.; Hampson, R. F., Jr.; Kerr, J. A.; Rossi, M. J.; Troe, J. *J. Phys. Chem. Ref. Data* **1997**, *26*, 521. (c) DeMore, W. B.; Sander, S. P.; Golden, D. M.; Hampson, R. F.; Kurylo, M. J.; Howard, C. J.; Ravishankara, A. R.; Kolb, C. E.; Molina, M. J. *JPL Publication* 97−4 **1997**. (d) Taylor, P. H.; Rahman, M. S.; Arif, M.; Dellinger, B.; Marshall, P. *Symp. Int. Combust. Proc.* **1996**, *26*, 497. (e) Wallington, T. J.; Hurley, M. D. *Environ. Sci. Technol.* **1993**, *27*, 1448. (f) Francisco, J. S. *J. Chem. Phys.* **1992**, *96*, 7597. (g) Libuda, H. G.; Zabel, F.; Fink, E. H.; Becker, K. H. *J. Phys. Chem.* **1990**, *94*, 5860 and references therein.

(4) The NIST Chemical Kinetics Database, NIST Standard Reference Database, U.S. Department of Commerce, Technology Administration, National Institute of Standards and Technology: Gaithersburg, MD, 17−2Q98.

(5) (a) Alvarez-Idaboy, J. R.; Mora-Diez, N.; Boyd, R. J.; Vivier-Bunge, A. *J. Am. Chem. Soc.* **2001**, *123*, 2018. (b) Mora-Diez, N.; Alvarez-Idaboy, J. R.; Boyd, R. J. *J. Phys. Chem. A* **2001**, *105*, 9034.

(6) (a) Wallington, T. J.; Hurley, M. D.; Ball, J. C.; Kaiser, E. W. *Environ. Sci. Technol.* **1992**, *26*, 1318. (b) Hasson, A. S.; Moore, C. M.; Smith, I. W. M. *Int. J. Chem. Kinet.* **1998**, *30*, 541. (c) Sanhueza, E. C.; Heicklen, J. *J. Phys. Chem.* **1975**, *79*, 7. (d) Gay, B. W.; Hanst, P. L.; Bufalini, J. J.; Noonan, R. C. *Environ. Sci. Technol.* **1976**, *10*, 58. (e) Niki, H.; Maker, P. D.; Savage, C. M.; Breitenbach, L. P. *Int. J. Chem. Kinet.* **1980**, *12*, 1001. (f) Niki, H.; Maker, P. D.; Savage, C. M.; Breitenbach, L. P.; Martinez, R. I.; Herron J. T. *J. Phys. Chem.* **1982**, *86*, 1858. (g) Tuazon, E. C.; Atkinson R.; Aschmann, S. M.; Goodman, M. A.; Winer, A. M. *Int. J. Chem. Kinet.* **1988**, *20*, 241. (h) Fantechi, G.; Jensen, N. R.; Saastad, O.; Hjorth, J.; Peeters, J. *J. Atmos. Chem.* **1998**, *31*, 247.

(7) (a) Eyring, H. *J. Chem. Phys.* **1935**, *3*, 107. (b) Evans, M. G., Polanyi, M. *Trans. Faraday Soc.* **1935**, *31*, 875.

(8) (a) Eckart, C. *Phys. Rev.* **1930**, *35*, 1303. (b) Shin, H. *J. Chem. Phys.* **1963**, *39*, 2934.

(9) Noxon, J. F.; Norton, R. B.; Henderson, W. R. *J. Geophys. Res.* **1978**, *5*, 675.

(10) (a) Noxon, J. F.; Norton, R. B.; Marovich, E. *Geophys. Res. Lett.* **1980**, *7*, 125. (b) Platt, U.; Perner, D.; Winer, A. M.; Harris, G. W.; Pitts, N. J. *Geophys. Res. Lett.* **1980**, *7*, 89.

(11) Atkinson, R. *Atmos. Environ.* **2000**, *34*, 2063.

(12) (a) Seinfeld, J. H. *Science* **1989**, *243*, 745. (b) Schwartz, S. E. *Science* **1989**, *243*, 753. (c) McElroy, M. B.; Salawitch, R. J. *Science* **1989**, *243*, 763. (d) Atkinson, R.; Plum, C. N.; Carter, W. P. L.; Winer, A. M.; Pitts, J. N., Jr. *J. Phys. Chem.* **1984**, *88*, 2361. (e) Calvert, J. G.; Stockwell, W. R. *Environ. Sci. Technol.* **1983**, *17*, 428A.

(13) (a) Cantrell, C. A.; Davidson, J. A.; Busarow, K. L.; Calvert, J. G. *J. Geophys. Res.* **1986**, *91*, 5347. (b) Louw, R.; van Harm, J.; Nieboer, H. *J. Air Pollut. Control Assoc.* **1973**, *23*, 716.

(14) Bandow, H.; Okuda, M.; Akimoto, H. *J. Phys. Chem.* **1980**, *84*, 3604.

(15) Wayne, R. P.; Barnes, I.; Biggs, P.; Burrows, J. P.; Canosa-Mas, C. E.; Hjorth, J.; Le Bras, G.; Moortgat, G. K.; Perner, D.; Poulet, G.; Restelli, G.; Sidebottom, H. *Atmos. Environ.* **1991**, *25A*, 1.

(16) (a) D'Anna, B.; Nielsen, C. J. *J. Chem. Soc., Faraday Trans.* **1997**, *93*, 3479. (b) Monks, P. S.; Stief, L. J.; Krauss, M.; Kuo, S. C.; Zhang, Z.; Klemm, R. B. *J. Phys. Chem.* **1994**, *98*, 10017.

(17) (a) Pérez-Casany, M.; Sánchez-Marín, J.; Nebot-Gil, I. *J. Am. Chem. Soc.* **2000**, *122*, 11585. (b) Pérez-Casany, M.; Nebot-Gil, I.; Sánchez-Marín, J. *J. Phys. Chem. A* **2000**, *104*, 6277, 10721, 11340. (c) King, M. D.; Canosa-Mas, C. E.; Wayne, R. P. *Phys. Chem. Chem. Phys.* **1999**, *1*, 2231, 2239. (d) Martínez E.; Cabañas, B.; Aranda, A.; Martín, P.; Salgado, S. *J. Atmos. Chem.* **1999**, *33*, 265. (e) Martínez E.; Cabañas, B.; Aranda, A.; Martín, P.; Salgado, S. *J. Phys. Chem. A* **1999**, *103*, 5321. (f) Fantechi, G.; Jensen, N. R.; Hjorth, J.; Peeters, J. *Atmos. Environ.* **1998**, *32*, 3547. (g) Pérez-Casany, M.; Nebot-Gil, I.; Sánchez-Marín, J. *J. Org. Chem.* **1998**, *63*, 6978. (h) Chew, A. A.; Atkinson, R.; Aschmann, S. M *J. Chem. Soc., Faraday Trans.* **1998**, *94*, 1083. (i) Noremsaune, I. M. W.; Langer, S.; Ljungström, E.; Nielsen, C. J. *J. Chem. Soc., Faraday Trans.* **1997**, *93*, 525. (j) Hallquist, M.; Langer, S.; Ljungström, E.; Wängberg, I. *Int. J. Chem. Kinet.* **1996**, *28*, 467. (k) Martínez E.; Cabañas, B.; Aranda, A.; Wayne, R. P. *J. Chem. Soc., Faraday Trans.* **1996**, *92*, 53, 4385. (l) Berndt, T.; Boge, O. *J. Atmos. Chem.* **1995**, *21*, 275. (m) Galan, B. C.; Marston, G.; Wayne, R. P. *J. Chem. Soc., Faraday Trans.* **1995**, *91*, 1185. (n) Skov, H.; Benter, T.; Schindler, R. N.; Hjorth, J.; Restelli, G. *Atmosph. Environ.* **1994**, *28*, 1583. (o) Grosjean, D.; Williams, E. *Atmos. Environ.* **1992**, *26A*, 1395.

(18) (a) Langer, S.; Ljungström, E. *J. Chem. Soc., Faraday Trans.* **1995**, *91*, 405. (b) Langer, S.; Ljungström, E. *Int. J. Chem. Kinet.* **1994**, *26*, 367.

(19) (a) Cabañas, B.; Salgado, S.; Martín, P.; Baeza, M. T.; Martínez E. *J. Phys. Chem. A* **2001**, *105*, 4440. (b) Papagni, C.; Arey, J.; Atkinson, R. *Int. J. Chem. Kinet.* **2000**, *32*, 79. (c) Ullerstam, M.; Langer, S.; Ljungström, E. *Int. J. Chem. Kinet.* **2000**, *32*, 294. (d) Alvarado, A.; Arey, J.; Atkinson, R. *J. Atmos. Chem.* **1998**, *31*, 281. (e) Glasius, M.; Calogirou, A.; Jensen, N. R.; Hjorth, J.; Nielsen, C. J. *Int. J. Chem. Kinet.* **1997**, *29*, 527. (f) Hallquist, M.; Wängberg, I.; Ljungström, E. *Environ. Sci. Technol.* **1997**, *31*, 3166.

(20) (a) Atkinson, R. *J. Phys. Chem. Ref. Data* **1991**, *20*, 459. (b) Hjorth, J.; Ottobrini, G.; Restelli, G. *J. Phys. Chem.* **1988**, *92*, 2669. (c) Cantrell, C. A.; Stockwell, W. R.; Anderson, L. G.; Busarow, K. L.; Perner, D.; Schmeltekopf, A.; Calvert, J. G.; Johnston, H. S. *J. Phys. Chem.* **1985**, *89*, 139. (d) Atkinson, R.; Plum, C. N.; Carter, W. P. L.; Winer, A. M.; Pitts, J. N., Jr. *J. Phys. Chem.* **1984**, *88*, 1210, 4446 (correction).

(21) (a) D'Anna, B.; Langer, S.; Ljungström, E.; Nielsen, C. J.; Ullerstam, M. *Phys. Chem. Chem. Phys.* **2001**, *3*, 1631. (b) Dlugokencky, E. J.; Howard, C. J. *J. Phys. Chem.* **1989**, *93*, 1091. (c) Morris, E. D., Jr.; Niki, H. *J. Phys. Chem.* **1974**, *78*, 1337.

(22) Frisch, M. J.; Trucks, G. W.; Schlegel, H. B.; Scuseria, G. E.; Robb, M. A.; Cheeseman, J. R.; Zakrzewski, V. G.; Montgomery, J. A., Jr.; Stratmann, R. E.; Burant, J. C.; Dapprich, S.; Millam, J. M.; Daniels, A. D.; Kudin, K. N.; Strain, M. C.; Farkas, O.; Tomasi, J.; Barone, V.; Cossi, M.; Cammi, R.; Mennucci, B.; Pomelli, C.; Adamo, C.; Clifford, S.; Ochterski, J.; Petersson, G. A.; Ayala, P. Y.; Cui, Q.; Morokuma, K.; Malick, D. K.; Rabuck, A. D.; Raghavachari, K.; Foresman, J. B.; Cioslowski, J.; Ortiz, J. V.; Stefanov, B. B.; Liu, G.; Liashenko, A.; Piskorz, P.; Komaromi, I.; Gomperts, R.; Martin, R. L.; Fox, D. J.; Keith, T.; Al-Laham, M. A.; Peng, C. Y.; Nanayakkara, A.; Gonzalez, C.; Challacombe, M.; Gill, P. M. W.; Johnson, B. G.; Chen, W.; Wong, M. W.; Andres, J. L.; Head-Gordon, M.; Replogle, E. S.; Pople, J. A. *Gaussian 98*, Gaussian, Inc.: Pittsburgh, PA, 1998.

(23) Frisch, A.; Frisch, M. J. *Gaussian 98 User's Reference*; Gaussian Inc.: Pittsburgh, PA, 1998; p 65.

(24) Mora-Diez, N.; Boyd, R. J., in preparation.

(25) (a) Zhang, Q.; Bell, R.; Truong, T. N. *J. Phys. Chem.* **1995**, *99*, 592. (b) Durant, J. L. *Chem. Phys. Lett.* **1996**, *256*, 595.

(26) Brown, R. L. *J. Res. Nat. Bur. Stand. (U.S.)* **1981**, *86*, 357.

(27) (a) Kawaguchi, K.; Ishiwata, T.; Hirota, E.; Tanaka, I. *Chem. Phys.* **1998**, *231*, 193. (b) Wang, D.; Jiang, P.; Qian, X.; Hong, G. *J. Chem. Phys.* **1997**, *106*, 3003. (c) Ishiwata, T.; Tanaka, I.; Kawaguchi, K.; Hirota, E. *J. Mol. Spectrosc.* **1992**, *153*, 167. (d) Kawaguchi, K.; Ishiwata, T.; Tanaka, I.; Hirota, E. *Chem. Phys. Lett.* **1991**, *180*, 436. (e) Hirota, E.; Kawaguchi, K.; Ishiwata, T.; Tanaka, I. *J. Chem. Phys.* **1991**, *95*, 771. (f) Weaver, A.; Arnold, D. W.; Bradforth, S. E.; Neumark, D. M. *J. Chem. Phys.* **1991**, *94*, 1740. (g) Kawaguchi, K.; Hirota, E.; Ishiwata, T.; Tanaka, I. *J. Chem. Phys.* **1990**, *93*, 951. (h) Friedl, R. R.; Sander, S. P. *J. Phys. Chem.* **1987**, *91*, 2721. (i) Ishiwata, T.; Tanaka, I.; Kawaguchi, K.; Hirota, E. *J. Chem. Phys.* **1985**, *82*, 2196. (j) Reuveni, A.; Luz, Z. *J. Magn. Res.* **1976**, *23*, 271.

(28) (a) Eisfeld, W.; Morokuma, K. *J. Chem. Phys.* **2000**, *113*, 5587. (b) Cao, X. Y.; Hong, G. Y.; Wang, D. X.; Li, L. M.; Xu, G. X. *Chin. J. Chem.* **2000**, *18*, 267. (c) Sherril, C. D.; Lee, M. S.; Head-Gordon, M. *Chem. Phys. Lett.* **1999**, *302*, 425. (d) Mayer, M.; Cederbaum, L. S.; Köppel, H. *J. Chem. Phys.* **1994**, *100*, 899. (e) Stirling, A.; Pápai, I.; Mink, J.; Salahub, D. R. *J. Chem. Phys.* **1994**, *100*, 2910. (f) Stanton, J. F.; Gauss, J.; Bartlett, R. J. *J. Chem. Phys.* **1992**, *97*, 5554. (g) Kaldor, U. *Chem. Phys. Lett.* **1991**, *185*, 131. (h) Kaldor, U. *Chem. Phys. Lett.* **1990**, *166*, 599. (i) Ishiwata, T.; Fujiwara, L.; Nagure, Y.; Obi, K.; Tanaka, I. *J. Phys. Chem.* **1983**, *87*, 1349. (j) Lund. A.; Thuomas, K.-Å. *Chem. Phys. Lett.* **1976**, *44*, 569.

(29) (a) Crawford, T. D.; Lee, T. J.; Handy, N. C.; Schaefer, H. F., III. *J. Chem. Phys.* **1997**, *107*, 9980. (b) Eriksson, L. A.; Wang, J.; Boyd, R. J.; Lunell, S. *J. Phys. Chem.* **1994**, *98*, 792. (c) Stanton, J. F.; Gauss, J.; Bartlett, R. J. *J. Chem. Phys.* **1991**, *94*, 4084. (d) Boehm, R. C.; Lohr, L. L. *J. Comput. Chem.* **1991**, *112*, 119. (e) Morris, V. R.; Bhatia, S.; Hall, J. H., Jr. *J. Phys. Chem.* **1991**, *95*, 9203. (f) Kim, B.; Hammond, B. L.; Lester, W. A., Jr.; Johnston, H. S. *Chem. Phys. Lett.* **1990**, *168*, 131. (g) Morris, V. R.; Bhatia, S.; Hall, J. H., Jr. *J. Phys. Chem.* **1990**, *94*, 7414. (h) Boehm, R. C.; Lohr, L. L. *J. Phys. Chem.* **1989**, *93*, 3430. (i) Davy, R. D.; Schaefer, H. F., III. *J. Chem. Phys.* **1989**, *91*, 4410. (j) Kim, B.; Johnston, H. S.; Clabo, D. A., Jr.; Schaefer, H. F., III. *J. Chem. Phys.* **1988**, *88*, 3204. (k) Siegbahn, P. E. M. *J. Comput. Chem.* **1985**, *6*, 182. (l) Baird, N. C.; Taylor, K. F. *Chem. Phys. Lett.* **1981**, *80*, 83. (m) Dewar, M. J. S.; Rzepa, H. S. *J. Am. Chem. Soc.* **1978**, *100*, 784. (n) Olsen, J. F.; Burnelle, L. *J. Am. Chem. Soc.* **1970**, *92*, 3659. (o) Chantry, G. W.; Horsfeld, A.; Morton, J. R.; Wiffen, D. H. *Mol. Phys.* **1962**, *5*, 589.

(30) (a) Löwdin, P.-O. *Rev. Mod. Phys.* **1963**, *35*, 496. (b) Löwdin, P.-O. *Adv. Chem. Phys.* **1969**, *14*, 283.

(31) Kestner, N. R.; Combariza, J. E. In *Reviews in Computational Chemistry*; Lipkowits, K. B., Boyd, D. B., Eds.; Wiley-VCH: New York, 1999; Vol. 13, p 99.

(32) (a) Boys, S. F.; Bernardi, F. *Mol. Phys.* **1970**, *19*, 553. (b) Handy, N. C.; Pople, J. A.; Shavitt, I. *J. Phys. Chem.* **1996**, *100*, 6007 (this paper gives a biographical synopsis on Boys' work). (c) Jansen, H. B.; Ros, P. *Chem. Phys. Lett.* **1969**, *3*, 140.

(33) Frisch, M. J.; Del Bene, J. E.; Binkley, J. S.; Schaefer, H. F., III. *J. Chem. Phys.* **1986**, *84*, 2279.

(34) Schwenke, D. W.; Truhlar, D. G. *J. Chem. Phys.* **1985**, *82*, 2418.

(35) For example, see: (a) Famulari, A.; Specchio, R.; Sironi, M.; Raimondi, M. *J. Chem. Phys.* **1998**, *108*, 3296. (b) Mayer, I.; Valiron, P. *J. Chem. Phys.* **1998**, *109*, 3360. (c) Surjan, P. R.; Mayer, I.; Lukovitz, I. *Chem. Phys. Lett.* **1983**, *119*, 538. (d) Pulay, P. *Chem. Phys. Lett.* **1983**, *100*, 1884.

(36) For example, see: (a) Vargas, R.; Garza, J.; Friesner, R. A.; Stern, H.; Hay, B. P.; Dixon, D. A. *J. Phys. Chem. A* **2001**, *105*, 4963. (b) Alagona, G.; Ghio, C.; Monti, S. *Int. J. Quantum Chem.* **2001**, *83*, 128. (c) Simon, S.; Bertran, J.; Sodupe, M. *J. Phys. Chem. A* **2001**, *105*, 4359. (d) Vargas, R.; Garza, J.; Dixon, D. A.; Hay, B. P. *J. Am. Chem. Soc.* **2000**, *122*, 4750. (e) Bolis, G.; Clementi, E.; Wertz, D. N.; Scheraga, H. A.; Tosi, C. *J. Am. Chem. Soc.* **1983**, *105*, 355. (f) Petterson, L.; Wahlgren, U. *Chem. Phys.* **1982**, *69*, 185.

(37) Benson, S. W. *Thermochemical Kinetics*, 2nd ed., Wiley & Sons: New York, 1976, p 43.

(38) Chuang, Y.-Y.; Truhlar, D. G. *J. Chem. Phys.* **2000**, *112*, 1221.

(39) (a) Galano, A.; Alvarez-Idaboy, J. R.; Montero, L. A.; Vivier-Bunge, A. *J. Comput. Chem.* **2001**, *22*, 1138. (b) Alvarez-Idaboy, J. R.; Mora-Diez, N.; Boyd, R. J.; Vivier-Bunge, A. *J. Am. Chem. Soc.* **2000**, *122*, 3715.

(40) Atkins, P. W. *Physical Chemistry*; Oxford University Press: New York, 1998.